AIChE WILEY InterScience DISCOVER SOMETHING GREAT

PARTICLE TECHNOLOGY AND FLUIDIZATION

Time-Dependent Behavior of a Catalyst in a Fluidized Bed/Cyclone Circulation System

Cornelis Klett, Ernst-Ulrich Hartge, and Joachim Werther
Institute of Solids Process Engineering and Particle Technology, Hamburg University of Technology, D 21071 Hamburg, Germany

DOI 10.1002/aic.11130
Published online February 27, 2007 in Wiley InterScience (www.interscience.wiley.com).

The performance of a catalytic fluidized-bed reactor is strongly dependent on the properties of the catalyst of which the particle-size distribution is one. The main influences on the particle-size distribution are attrition of the catalyst particles, and the classifying effect of the solids recovery system. In a fluidized-bed reactor a particle will be subjected to attrition due to different mechanisms in different parts of the system, namely attrition by gas jets near the bottom of the fluidized bed, bubble-induced attrition in the fluidized bed itself, and attrition during the passage through a cyclone. All these different attrition mechanisms are considered in this work by different mathematical models. It is known that a fresh catalyst is much more fragile and exhibits a much higher attrition rate at the beginning of exposure to mechanical stress than under steady-state conditions. Depending on the mechanism the particles need different times or in the case of attrition in a cyclone a certain number of passages to reach a constant value of the attrition rate. In the fluidized-bed system a particle will during its aging experience all the different attrition mechanisms. In order to summarize the effect of these stresses on the particle within the different parts of the fluidized-bed system, the concept of the "stress history" has been developed, which allows a uniform treatment of the different attrition mechanisms. This concept has been implemented into an existing population balance model. Experiments with a FCC-catalyst in a fluidized/bed-cyclone circulation system are well described by this model. © 2007 American Institute of Chemical Engineers *AIChE J,* 53: 769–779, 2007
Keywords: fluidized bed, attrition, modeling, cyclone

Introduction

For the operation of a fluidized-bed system consisting of a fluidized bed, and a solids recovery with recirculation of the entrained solids the particle-size distribution (PSD) of the bed material is an essential characteristic parameter besides operating conditions, such as gas velocity, pressure, temperature and geometry. The operating performance of fluidized-bed reactors is known to be significantly influenced by the PSD. For example, de Vries et al.[1] report that an increase in the conversion of gaseous hydrogen chloride in the Shell Chlorine process from 91% to 95.7% was achieved by increasing the fines content in the bed material from 7 to 20%. The same effect was observed by Pell and Jordan[2] with respect to the propylene conversion during the synthesis of acrylonitrile. They reported an increase of the conversion from 94.6% to 99.2% as the fines content was changed from 23% to 44%. Unfortunately, experiences with the application of fluidized beds in the chemical industry are seldom published. However, these two examples demonstrate the importance of the PSD in these processes.

Correspondence concerning this article should be addressed to E-U. Hartge at hartge@tuhh.de.

In addition to the reported industrial experiences there is scientific research available in the literature. There the influence of particle properties including their size on effects in fluidized-bed applications is investigated. Cheng et al.[3] investigated the sulfur capture capability of sorbents under fluidized-bed conditions, and found that the capture capability increases with increasing mass specific surface area. According to Hilligardt and Werther[4] the size of bubbles is decreasing with decreasing particle size. Consequently, the mass transfer from the bubble phase to the surrounding suspension is increased (Sit and Grace[5]), as well as the number of bubbles. As a result the conversion of a heterogeneously catalyzed gas-phase reaction is increased. This effect was demonstrated by Werther and Hartge[6] in model calculations where the influence of cyclone performance on a FCC-reactor was investigated.

From the aforementioned examples it is quite clear, that the PSD of the catalyst in a reactor plays an important role in the conversion of the reactants to the product. In general, the factors that are influencing the PSD in a fluidized-bed system with recirculation of solids can be divided into two groups. The first one consists of classification and separation effects while the second one comprises degradation effects, for example, fragmentation, shrinkage and attrition. In the scope of this work attrition means abrasion that is, shrinking of mother particles by chipping of much smaller daughter particles from the mother particle's surface. This process is understood to be the dominating effect leading to size reduction of catalyst particles in FCC reactors.

The loss of produced fines by the attrition of FCC catalyst results in operating costs. Therefore, a lot of research work in the past was focused on the development of less friable catalyst particles and techniques to classify them (for example, Forsythe and Hertwig[7]). More recently Xi[8] and Reppenhagen[9] developed experimental methods to measure the attrition rates of FCC catalyst independently for the different sources of attrition in a fluidized-bed system. Xi investigated the attrition due to the gas jets at the gas distributor and the bubble-induced motion within a fluidized bed. The findings of Xi were extended by Reppenhagen[9] who studied the attrition in cyclones.

All these investigations have been evaluated only when the attrition rate had reached a constant value and ignored the significantly higher-attrition rate for fresh particles. However, catalyst attrition is in fact a time-dependent process (Werther and Reppenhagen[10]). For example, Gwyn[11] described his experiments in a small-scale test apparatus by

$$\frac{m_{elutriated}}{m_{bed,0}} = K_a \cdot t^{b^*} \tag{1}$$

where $m_{elutriated}$ denotes the elutriated catalyst mass at the time t, and $m_{bed,0}$ is the bed mass at $t = 0$. The parameter b^* was constant for different samples of the same catalyst, whereas the attrition constant K_a decreased with mean-particle size. Other empirical correlations of the same type were suggested by Pis et al.[12] and Dessalces et al.[13]. The disadvantage of such correlations is that they are restricted to the special equipment and operating conditions from which they were derived. Because of these restrictions a direct transfer to other equipment and scaleup is not easily possible.

In this article an attempt is, therefore, made to describe the time-dependence of attrition separately for the different attrition mechanisms occurring in the system. Based on experimental results a stress history parameter is introduced, which permits a generalized description of the fate of the catalyst particle in the system. The simulation is confirmed by measurements in a cold model setup with FCC-catalyst particles.

Theory

General strategy for modeling the particle-size distribution in a fluidized-bed system with recirculation of solids

A fluidized-bed system can consist of a combination of fluidized beds, cyclones and return lines. A simple combination is presented in Figure 1. It is wise to subdivide the model into modules, when a flexible model is desired for the description of effects concerning the PSD of the solids in the system. Each module describes one single apparatus of the system and provides an interface for the transfer of the streams between the modules. The modules defined here are the fluidized bed, the cyclone and the return line. The particle-size relevant effects considered in the modules are attrition and classification.

The return line is modeled as a standpipe, where solids can be accumulated. It is assumed that the governing flow regime is of plug flow. The accumulation has an influence on time-dependent effects. Besides the return line module only the fluidized-bed module is capable of accumulating solids. In the cyclone it is assumed that solids accumulation is negligible.

The dynamic calculation of the a system is realized in such a way that the modules are initialized with defined conditions, for example, mass of inventory, particle-size distribution, stress-history distribution, kind of solids and model specific parameters, and so on. Then the modules are computed sequentially with prefixed time steps of length Δt, until either steady-state is reached or a total operating time has elapsed.

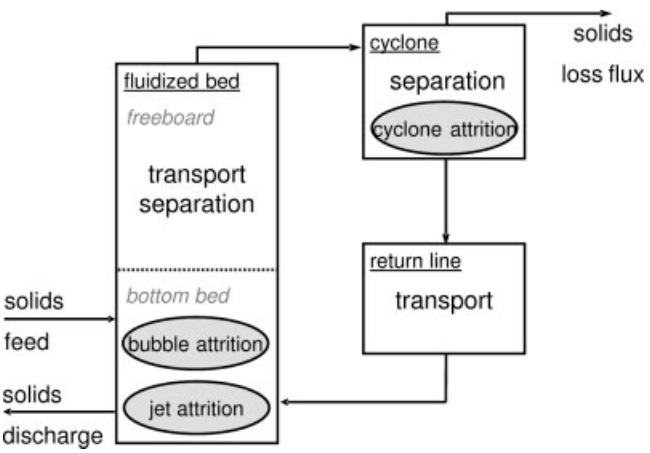

Figure 1. Example of the model layout of a fluidized-bed system with recirculation of solids.

Change of particle-size distribution by attrition

The mass balance for one class i which ranges from x_{i-1} to x_i can be written as follows

$$\frac{dm_i}{dt} = -\dot{m}_{att,i} - \dot{m}_{i,i-1} + \dot{m}_{i+1,i} \tag{2}$$

The loss of mass in the class i leaving the class as produced fines is $\dot{m}_{att,i}$. The production of fines leads to the shrinkage of particles which causes some particles to shrink from class i to class $i - 1$. This mass which is moving across the boundary from class i to class $i - 1$ per unit time is the mass flow rate $\dot{m}_{i,i-1}$.

With the assumption of an even distribution of mass within the size interval between x_{i-1} and x_i the mass of solids traveling from class i to class $i - 1$ is

$$m_{i,i-1} = (m_i - m_{att,i}) \cdot \frac{x_i^* - x_{i-1}}{x_i - x_{i-1}} \tag{3}$$

x_i* is the diameter of the biggest particle which will shrink enough to move from class i to class $i - 1$ within the time interval Δt. The mass $m_{p,i}^*$ of the particle with size x_i* can be determined by solving the mass balance at a single particle (index p)

$$m_{p,i}^* = m_{p,i-1} + r_i \cdot \Delta t \cdot m_{p,i}^* \tag{4}$$

r_i is a mass related attrition rate for the particles in class i with the approximation that the attrition rate is equal for all particles within the class I, and is defined as follows

$$r_i = \frac{\dot{m}_{att,i}}{m_i} \tag{5}$$

The attrition rate r_i is dependent on the source of attrition, operating conditions, solids properties and the state (or age) of the particles. The definition and calculation of r_i will be explained in the following section.

Equation 4 can be written as

$$x_i^{*3} = x_{i-1}^3 + r_i \cdot \Delta t \cdot x_i^{*3} \tag{6}$$

and x_i* is then calculated by

$$x_i^* = \frac{x_{i-1}}{\sqrt[3]{1 - r_i \cdot \Delta t}} \tag{7}$$

Time-dependence of attrition

The typical development of the production of fines with time is sketched in Figure 2. The time-dependent behavior is found for jet-induced attrition and bubble-induced attrition. For attrition in cyclones the attrition rate will depend on the number of passes. When an experiment is started with fresh particles which have not undergone attrition before, the production rate of fines is high at the beginning. During operation it decreases and finally approaches a constant rate.

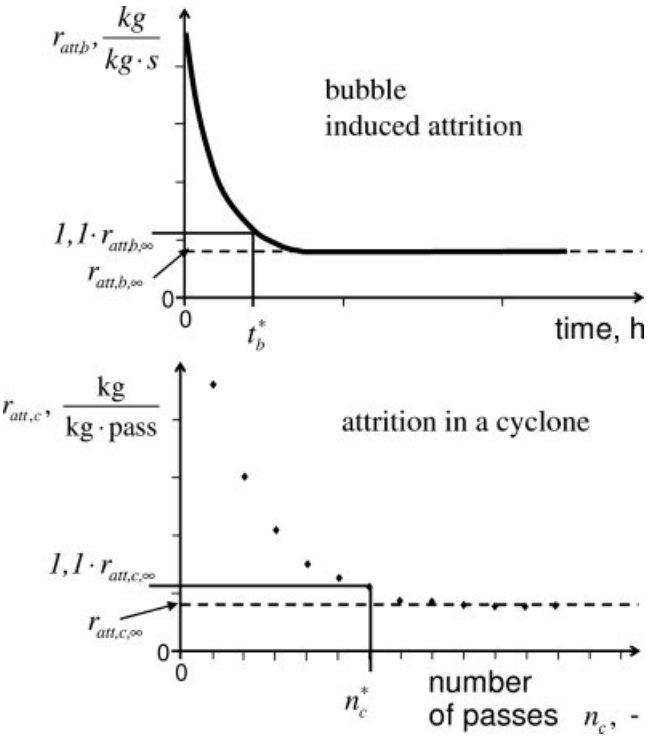

Figure 2. Qualitative development of attrition rate, due to bubbles with time and inside a cyclone as a function of number of passes with definitions of the characteristic parameters t_b^* for the case of bubble induced attrition and n_c^* for attrition in cyclones.

The picture for jet-induced attrition is similar to that of bubble-induced attrition.

The dependence of the steady-state attrition rate r_∞ on operating conditions and material properties was investigated and modeled in previous work (Werther and Xi,[14] Werther and Reppenhagen,[15] Reppenhagen and Werther[16]). r_∞ is the production rate of fines $\dot{m}_{att\infty}$ related to the mass of solids exposed to the respective stress. $\dot{m}_{att\infty}$ under steady-state conditions can be described for all sources of attrition by the following relationship

$$\dot{m}_{att,\infty} = C^* \cdot d_p \cdot \xi^* \quad |\xi^* = \xi_b, \xi_j, \xi_c; \quad C^* = C_b, C_j, C_c \tag{8}$$

Here, the attrition at steady-state conditions is calculated as the product of a solids related attrition coefficient C*, a characteristic mean-particle diameter (that is, surface mean diameter) d_p, and a parameter ξ* which is taking the respective operating conditions into account (Reppenhagen and Werther[16])

$$\begin{aligned} \xi_b &= m_b \cdot (u - u_{mf})^3 \\ \xi_j &= \rho_f \cdot d_{or}^2 \cdot u_{or}^3 \cdot n_{or} \\ \xi_c &= \dot{m}_{c,in} \cdot u_{c,in}^2 / \sqrt{\mu_{c,in}} \end{aligned} \tag{9}$$

It was found that the production of fines is proportional to the surface-mean diameter of the particle-size distribution

(Reppenhagen and Werther[16]), which means that the total production mass rate of fines can be calculated as

$$\dot{m}_{att,\infty} = \sum \dot{m}_{att,\infty,i} = C^* \cdot \xi^* \cdot \sum \bar{x}_i \cdot \Delta Q_{2,i} \tag{10}$$

where $Q_{2,i}$ is the cumulative distribution of particle surface. $\Delta Q_{2,i}$ is the ratio of particle surface contained in the interval i to the entire particle surface. The production rate of fines within one class i is

$$\dot{m}_{att,\infty,i} = C^* \cdot \xi^* \cdot \bar{x}_i \cdot \Delta Q_{2,i} \tag{11}$$

For one class i the attrition rate $r_{\infty,i}$ is then

$$r_{\infty,i} = \frac{\dot{m}_{att,\infty,i}}{m_i} = \frac{C^* \cdot \xi^*}{m_{tot}} \cdot \bar{x}_i \cdot \frac{\Delta Q_{2,i}}{\Delta Q_{3,i}} \tag{12}$$

As is seen from experiments the attrition rate depends not only on operating conditions and material properties, but also on the state of the particles. The instantaneous state of the particle and its history plays an important role for the attrition rate. When the surface of the particles is not yet smoothed they will produce much more fines than under steady-state conditions.

Moreover, when more than one source of attrition is present in a given system it is not easy to determine the condition of the particles surface at a given time. As an example, consider a simple system consisting of a fluidized bed, a cyclone and a return leg, using particles with a density of 1,500 kg/m^3. The fluidized bed is operated with air at ambient temperature and pressure at a superficial velocity of 0.3 m/s. The PSD of the particles contains sizes ranging from 40 to 150 μm, from which we will take a look at both the particles of size 100 μm and of 60 μm. The 100 μm particles have a terminal velocity of approximately 0.45 m/s, which is greater than the fluidizing velocity. This would mean that these particles will hardly be elutriated and never be exposed to attrition in the cyclone. On the other hand the 60 μm particles have a terminal velocity of about 0.16 m/s. They are easily entrained and will pass the cyclone several times where they will undergo attrition, be separated from the gas stream and be returned to the fluidized bed again. The 60 μm particles will, therefore, be exposed not only to the abrasive conditions in the fluidized bed, but also to the abrasive conditions in the cyclone in a given period of time. The actual attrition rate after 1 h of the 100 μm particles can then easily be taken from the measured time-dependence of the attrition rate in the fluidized bed. On the other hand, the actual attrition rate of the smaller 60 μm particles will certainly depend on the number of passages through the cyclone they experienced besides the bubble-induced attrition they underwent during their stay in the bed. In this case a description is needed which considers the complex "stress history" of the particles.

In order to obtain a more general description of the attrition process, characteristic states are defined for the different attrition mechanisms. These are the steady states which are characterized by the attrition rates. The steady state is, however, only reached asymptotically. For convenience a characteristic time t^* is defined which is needed to reach an attrition rate r^* of $1.1 \cdot r_\infty$. This is also illustrated in Figure 2.

A similar procedure is applied for attrition in cyclones with the difference that the attrition in cyclones is not time-dependent, but depending on the number of passes n_c through the cyclone. Therefore, the characteristic value is called n_c^*. Based on the characteristic values t_b^*, t_j^* or n_c^* a stress history variable ϑ is now defined by

$$\begin{aligned} \vartheta_b &= t/t_b^* \quad \text{for in-bed attrition} \\ \vartheta_c &= n_c/n_c^* \quad \text{for attrition in cyclones} \\ \vartheta_j &= t/t_j^* \quad \text{for jet-induced attrition} \end{aligned} \tag{13}$$

In a fluidized-bed system with solids recirculation, particles with different sizes have different residence times in different regions of the system. In such a system the stress histories for the different mechanisms are linked, for example, stress which the particle has experienced in the cyclone will also influence the subsequent attrition rate due to bubbles. For simplicity it is assumed that the stresses which the particles experience due to the different mechanisms can be added

$$\vartheta = \vartheta_b + \vartheta_j + \vartheta_c \tag{14}$$

A uniform description of stress for all three attrition mechanisms should be possible by

$$r_i(\vartheta) = f(\vartheta) \cdot r_{\infty,i} \tag{15}$$

with $r_{\infty,i}$ calculated from Eq 12. The influence of the experienced stress history is considered here by the factor $f(\vartheta)$. Equation 14 implies the assumption that the function $f(\vartheta)$ is independent of the particle size. $f(\vartheta)$ has to be determined from experiments.

With the introduction of ϑ as the stress-history parameter a second dimension for the solids property besides their size has been added. This has to be considered in calculations. In order to take into account of the different stress histories of particles, the mass of particles in each size class is assumed to be distributed over several stress-history classes with ϑ_j as the upper bound of class j. Particles are then transferred according to their individual stress from stress-history classes with small ϑ to classes with larger ϑ. The mass transferred within a time step Δt in the bed, or in the jet or during one pass through the cyclone from class j to class $j+1$ is

$$m_{j,j+1} = m_j \cdot \frac{\Delta\vartheta}{\vartheta_{j+1} - \vartheta_j} \tag{16}$$

The equation assumes that particles are evenly distributed in the interval between ϑ_j and ϑ_{j+1} and $\Delta\vartheta$ is describing the aging of material during one time step Δt, or during one pass through the cyclone, respectively. $\Delta\vartheta$ for the individual sources can be calculated as follows

$$\Delta\vartheta_b = \Delta t/t_b^*, \quad \Delta\vartheta_j = \Delta t/t_j^*, \quad \Delta\vartheta_c = 1/n_c^* \tag{17}$$

The values for t_b^* and n_c^* are directly determined from experiments. Since a jet stresses only a limited amount of solids during one time step, the time until the whole bed mass will reach steady-state conditions will depend on the ratio of the bed mass to the number of jets. Thus, the value of t_j^* for the simulation of a system with an inventory and a

number of jets which differs from the conditions under which $t^*_{j,\mathrm{exp}}$ was experimentally determined is obtained from

$$t^*_j = t^*_{j,\mathrm{exp}.} \cdot \frac{m_b}{m_{b,exp,j}} \cdot \frac{n_{or,exp}}{n_{or}} \tag{18}$$

Here $m_{b,exp.}$ and $n_{or,exp.}$ are the mass of bed material and number of jets in the experimental determination of $t^*_{j,exp}$, respectively. m_b and n_{or} represent the mass of bed material and number of jets for the simulation conditions.

Classification

There are two different classifying effects present in a system with recirculation of solids, one is the entrainment of small particles from the bed material in the fluidized bed, and the other is the effect which occurs in the cyclone.

The fluidized bed itself is modeled by the two-phase model by Werther and Wein.[17] The mass flow entrained from the fluidized bed is calculated for each class by

$$m_{e,i} = k_{\infty,i} \cdot \Delta Q_{3,bed,i} \cdot \Delta t \cdot A_t \tag{19}$$

with $k_{\infty,i}$ being a particle size related entrainment coefficient with the dimension of kg/m^2/s. A large number of correlations are available to determine $k_{\infty,i}$. In this work the one by Tasirin and Geldart[18] has been used

$$k_{\infty,i}\left[\frac{\mathrm{kg}}{\mathrm{m^2 s}}\right] = \begin{cases} 23.7 \cdot \rho_f \cdot u^{2.5} \exp\left(-5.4\,\dfrac{w_{s,i}}{u}\right) & \text{for } \mathrm{Re} < 3000 \\ 14.5 \cdot \rho_f \cdot u^{2.5} \exp\left(-5.4\,\dfrac{w_{s,i}}{u}\right) & \text{for } \mathrm{Re} > 3000 \end{cases} \tag{20}$$

with

$$\mathrm{Re} = \frac{D_t \cdot u \cdot \rho_f}{\eta_f}. \tag{21}$$

For the simulation of the separation of the solids from the gas in a cyclone, the model by Trefz and Muschelknautz[19] and Muschelknautz et al.[20] which is commonly used in Germany in industrial application and design procedures has been adopted. According to Muschelknautz et al.[20] two effects are causing the separation of the solids from the gas, one being the classification in the vortex due to the centrifugal forces, while the other is due to the limited solids carrying capacity of the gas flow. This latter separation which is associated with a strand forming on the wall takes place at the inlet. For solids loadings $\mu_{c,in}$ higher than a critical loading μ_{cr} a solids mass corresponding to $(\mu_{c,in} - \mu_{cr})$ is separated from the flow in the form of strands. Only the mass fraction limited by μ_{cr} enters the inner vortex. The solid loading $\mu_{c,in}$ is the ratio of solids-mass flow to gas-mass flow in the cyclone inlet. In the original model (Muschelknautz et al.[20]) the PSD of the particles passing the inlet separation into the inner vortex is approximated by a RRSB distribution. However, in terms of particle-class sizes this can lead to a violation of mass balances, when used in population balances. Therefore, in this work a nonclassifying separation at the cyclone inlet has been assumed.

Experimental

Experimental facilities

Determination of Attrition Related Material Characteristics. For the application of the earlier described attrition model to a fluidized bed the parameters C_b, C_c and C_j, which describe material characteristics are needed. They have to be determined in separate experiments. To investigate the attrition behavior of particles at the three sources (jets, bubble movement and cyclones) specific experimental setups have to be used, to ensure that the effects of the sources can be studied independently from each other (Werther and Reppenhagen,[10] Werther and Xi,[14] Reppenhagen and Werther[21]).

The experiments regarding attrition inside a fluidized bed were carried out in the facilities sketched in Figure 3. Two setups were available for the investigation of bubble-induced attrition. The left fluidized-bed column has an inner dia. of 0.2 m, and the right, 0.05 m. The two units are equipped with an expansion section at the top which acts as a gravitational separator by decreasing the gas velocity. The ratio of the diameter of the lower part to the diameter of the separator is the same for both columns.

At the beginning of each experiment a portion of fresh that is, non prestressed solids is put into the fluidized bed. The large column is filled with approximately 5 kg of material and the smaller one with about 0.25–0.5 kg. This leads to a bed height at minimum fluidization of 0.15–0.25 m, depending on the bulk density of the solids. The bed solids are sieved before the experiment to contain only particles with a terminal velocity greater than the cut velocity of the gravity separator at the operating velocity of the fluidized bed. This assures that the particles collected in the filter can be attributed to attrition. The bed is fluidized via a porous plate with pressurized air.

For running an experiment to obtain the jet-induced attrition characteristics the fluidized bed which is surrounding the jet is fluidized gently to ensure a homogeneous mixing of the

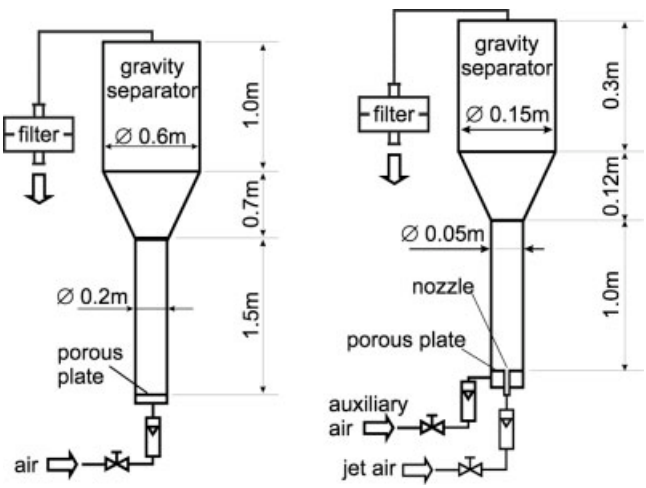

Figure 3. Setups for jet and bubble-induced attrition: left setup for bubble-induced attrition only and right for both attrition sources (diameters are inner dimensions).

material. The jet is formed by a nozzle with a single hole of 2 mm dia.

The entrained particles which were abraded from the mother particles were separated from the gas by fabric filters. Both of the plants had filter systems consisting of two filters with a two-way valve between. This allowed for continuous operation. For the larger plant, filter bags were applied which were weighed before and after the usage, and which were cleaned by back flushing with pressurized air. The smaller plant used paper filters which were dried and weighed before and after the usage, and were used only once. The solids collected on the filters were assumed to be only particles which were originating from attrition. From the measured mass of solids collected on the filter together with the known length of the time interval, an average mass flow of produced fines was obtained. This average mass flow was then attributed to the middle of the time interval.

The procedure for quantifying the cyclone-induced attrition was different. A portion of solids was stressed by passing through a cyclone several times. The fines produced were caught on a filter and weighed. The setup for the assessment is shown in Figure 4. Batches of the solids were fed into the inlet pipe of the cyclone via a vibration feeder. Inside the cyclone the particles were subjected to attrition, and the mother particles are separated and collected in the hopper below the underflow of the cyclone. The fines produced with diameters usually below 5 μm were entrained from the cyclone with the off-gas through the overflow, and then caught on the filter. Misled coarse particles were separated from the fines by a 25 μm sieve before the filter. After that the solids were taken from the collecting hopper and put back into the feeding hopper for the next run. The filters were the same paper filters as for the jet-induced attrition tests, and were used for up to 4 runs. After the runs the filter was taken out, dried and weighed. The mass increase of the filter was assumed to be due to produced fines and divided by the number of corresponding runs, and the sum of the masses fed during these runs. A mass related attrition rate with the dimension of kg/kg/run was obtained as the average attrition rate of these runs.

Operation of a fluidized bed-cyclone circulation system

The test facility shown in Figure 5 consisted of a 0.2 m dia. fluidized bed coupled with a cyclone and a recirculation line. The bed was operated as a bubbling-fluidized bed. The

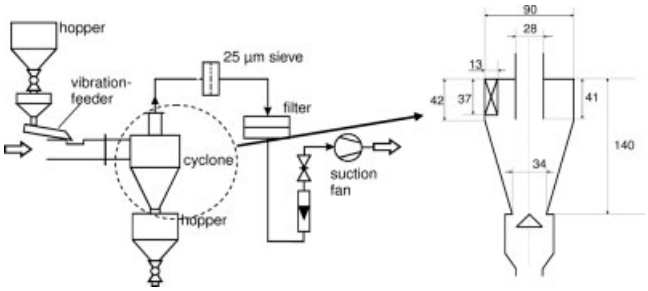

Figure 4. Experimental setup for the assessment of attrition in cyclones (dimensions are given in mm).

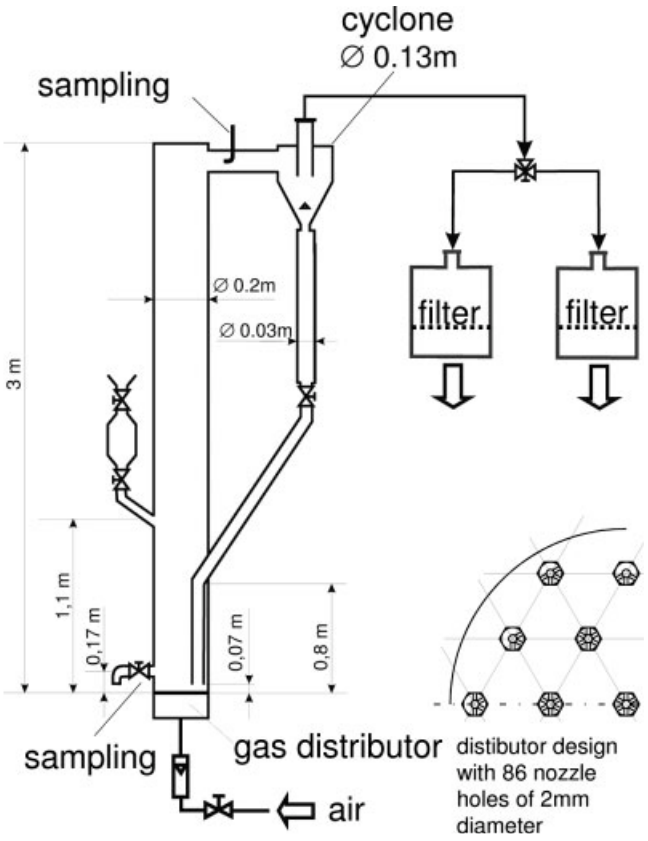

Figure 5. Bubbling-fluidized bed test plant.

gas distributor consisted of 86 nozzles. The nozzles had outlet openings with a diameter of 0.002 m. The solids recirculation from the cyclone was effected via a dipleg, which ended 0.07 m above the nozzles. In the inlet channel of the cyclone a port for a suction probe was provided where solid samples could be taken.

For taking samples from the bed a bottom drain was provided. Bigger portions of particles were taken and split by a sample splitter down to smaller samples of a few grams. The rest is given back to the system by a solids lock located at the height of 1.1 m. The solids which could not be kept in the system by the cyclone left with the overflow and were caught in a fabric bag filter. The filter system was configured with two filters which could be used alternately to allow continuous operation. By weighing the filters and dividing the increase in mass by the corresponding time interval the average loss rate was obtained and related to the middle of the time interval.

Catalysts used

Two types of catalysts were used in this work as examples. Both were typical FCC-catalysts (cf. Table 1 and Figure 6). The catalyst FCC-A was a spent catalyst obtained from a refinery. This catalyst had, thus, already undergone mechanical stress for a long time and may be assumed to be in steady state with respect to its resistance against attrition. On the other hand, the catalyst FCC-B was a fresh catalyst which had not yet experienced fluidized-bed operation.

Table 1. Solids properties for model calculations

	FCC A (spent)	FCC B (fresh)
density, kg/m^3	1550	1560
C_b, s^2/m^4	0.3 10^{-3}	0.48 10^{-3}
C_c, s^2/m^3	0.92 10^{-3}	1.9 10^{-3}
C_j, s^2/m^3	13.1 10^{-6}	12.2 10^{-6}
t_b^*, h	–	358
t_j^*, h	–	184
$m_{exp.j}$, kg	–	0.2
n_p^*, -	–	25
b, -	–	−1.16

Results and Discussion

Time-dependent attrition

In Figure 7 the measured attrition rate for the bubble-induced attrition of FCC-B is plotted as a function of time. The time-dependence of the production of fines is evident in this experiment. At the beginning a very high-mass flow of fines occurs which decreases with time to a nearly constant one. The attrition rate at the beginning is about two-orders of magnitude higher than at steady state. This is caused by the surface properties of fresh particles. The fines produced at the beginning originate from breaking edges and cracks. After a while the rough edges have vanished and the surface is smoothened to a natural roughness which will remain constant.

The time-dependence has been modeled by Eq. 26 with ϑ being given by Eq. 13. A least-squares fit yields for the experiments shown Figure 7 characteristic parameters

$$r_{b,\infty} = 6.3 \cdot 10^{-6}\ \text{kg/(kg h)}$$
$$t_b^* = 401\ \text{h}$$
$$b = -1.18$$

The development with time of the attrition rate for the jet-induced attrition in Figure 8 looks similar to the one for bubble-induced attrition. However, contrary to the bubble-induced attrition rate the jet-induced attrition rate cannot be measured independently. The fact that the bed surrounding the jet has to be fluidized causes additional attrition by bubble movement (Werther and Xi[14]). The attrition rate is the

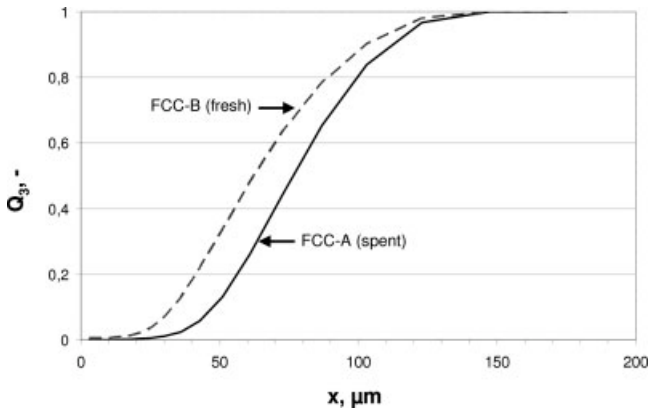

Figure 6. Particle-size distributions of the catalysts used in this work.

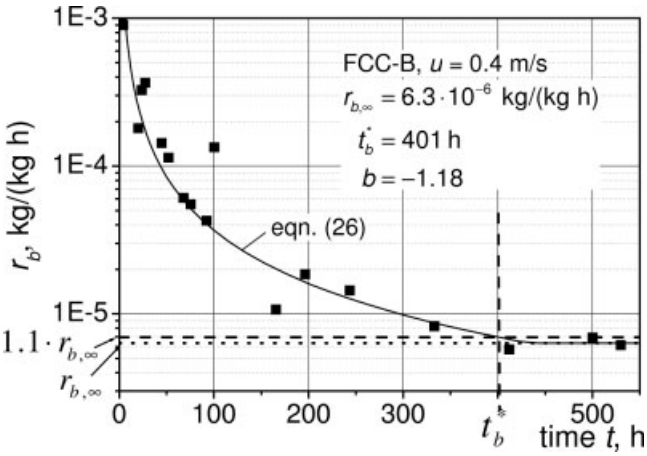

Figure 7. Time-dependence of bubble-induced attrition and determination of t_b^*.

sum of jet-induced attrition rate and the bubble-induced one. Therefore, the jet-induced attrition rate $r_{j,\infty}$ is obtained by simply subtracting the bubble-induced attrition rate $r_{b,\infty}$ from the measured total attrition rate. The attrition coefficient C_b can be calculated from Eq. 12 with the attrition rate $r_{b,\infty}$ obtained from the measurements shown in Figure 7.

From the plot in Figure 8, t_{tot}^* is determined in a similar way to t_b^*. It is called t_{tot}^* because this value also includes the effect of bubble-induced attrition in addition to the one induced by the jet. This results in a combined change of stress history by either bubbles, as well as the jet which cannot be measured separately. With the assumption that the stress histories can simply be added, the increase of ϑ within one time step is the sum of the increases induced by bubbles and jet, respectively

$$\Delta\vartheta_{tot} = \Delta\vartheta_b + \Delta\vartheta_j \tag{22}$$

In detail this relationship may be expressed by

$$\Delta\vartheta_{tot} = \frac{\Delta t}{t_{tot}^*} = \frac{\Delta t}{t_b^*} + \frac{\Delta t}{t_j^*} \tag{23}$$

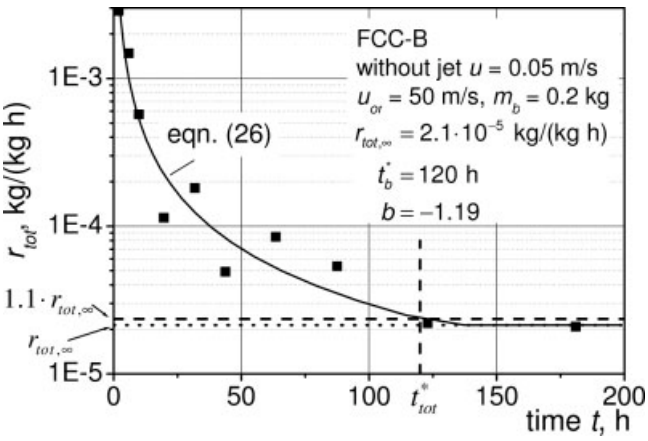

Figure 8. Time-dependence of jet-induced attrition and determination of t_{tot}^*.

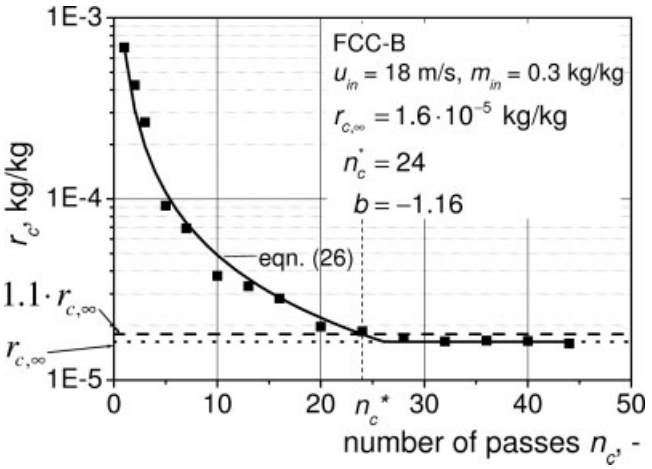

Figure 9. Dependence of attrition in cyclones on number of passes and determination of n_c^*.

Since the time step Δt is the same for all $\Delta\vartheta$ it follows

$$t_j^* = \left(\frac{1}{t_{tot}^*} - \frac{1}{t_b^*}\right)^{-1} \tag{24}$$

To complete the picture experiments conducted in cyclones were evaluated in a similar way. However, the attrition rate r_c is a function of the number of passes n_c through the cyclone rather than of time. Figure 9 shows the decrease of attrition rate r_c with increasing number of passes n_c. A summary of the characteristics which have been obtained for the two catalysts used in this work is given in Table 1.

Assuming that the functional dependence of the attrition rate on the stress history variable (which is defined in Eq. 15 for a size class i) is the same for all size classes, it follows

$$f(\vartheta) = \frac{r(\vartheta)}{r_\infty} \tag{25}$$

In Figure 10 the thus defined dimensionless attrition rate is plotted vs. ϑ for the fresh catalyst FCC-B. The dimensionless attrition rates for all experiments meet one curve with a fairly low deviation. In this double logarithmic plot the relation is approximated by a straight line for $\vartheta < 1$, and is constant for ϑ running toward infinity. Therefore, the stress history function may be described by

$$\frac{r(\vartheta)}{r_\infty} = f(\vartheta) = \begin{cases} 1.1 \cdot \vartheta^b & \text{for} \quad \vartheta \le (1/1.1)^{1/b} \\ 1 & \text{for} \quad \vartheta > (1/1.1)^{1/b} \end{cases} \tag{26}$$

The slope of the straight line is the stress history exponent b, which is found to be -1.16 for the FCC catalyst used here. The thus obtained numerical value of b depends on the material and structure of the catalyst particles[22] only.

Application of the model

The population balance model finally was applied to simulate two test runs in the cold fluidized bed system shown in Figure 5. While for the attrition tests the fines of the FCC catalyst with diameters less than 80 μm were removed by sieving, in the fluidized bed system the catalyst was used as received (cf. Figure 6). The first test run was conducted using the spent catalyst FCC-A. In this case the development with time of the PSD, and the mass loss of the system is affected by the steady-state attrition of the particles and the separation effects of the system; stress history can be neglected since the catalyst has already undergone mechanical stress in the commercial unit for a long time. FCC-B was used for the second test in the same test rig. In this latter test run the additional impact of the stress history of the particles comes into play, since the catalyst has not undergone mechanical stress before.

The test with the spent catalyst FCC-A was started with an initial inventory of the system of 6.5 kg. A fluidizing velocity of 0.3 m/s was applied. Under these conditions a velocity of 9 m/s at the cyclone inlet is generated. The development of the mass flux in the overflow of the cyclone to the filter is presented in Figure 11. The mass flux is seen to increase over a period of several days to a nearly constant value. The simulation which was based on the parameter values obtained in the previous attrition tests, with no fitting being possible gives a good portrayal of this development, even though the solids loss under stationary conditions is slightly underestimated by the simulation. The deviation at the beginning, that is, the slower increase of the measured loss flux may be due to the capacity of the fluidized bed to capture and accumulate fines. At the beginning the produced fines are not completely entrained from the bed, but due to interparticle forces stick to coarse particles and are, thus, kept within the bed. Another effect which may be contributing is the coating of metal surfaces in the freeboard, and in the tubing which occurs during the first days of operation, which also prevents fine particles from escaping from the system.

The very first data point does not fit into the general picture. The corresponding measurement was taken 40 min after startup. The calculated loss of 2.7 g/d corresponds to a solids mass collected on the filter of $7.5 \cdot 10^{-2}$ g only which is close to the limit of accuracy of the measurement setup. It is

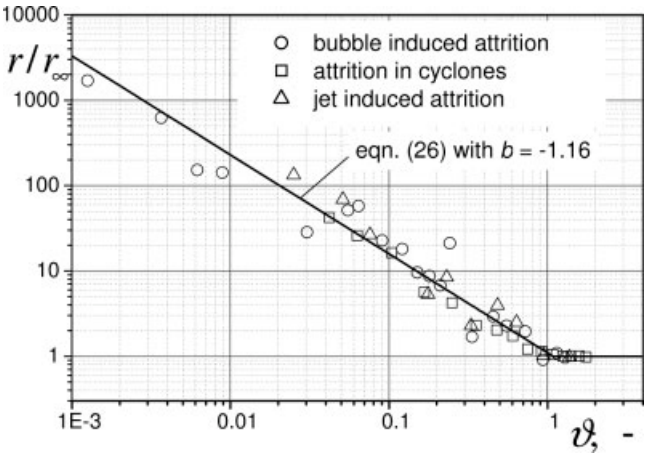

Figure 10. Dimensionless attrition rate of FCC-B as function of stress history.

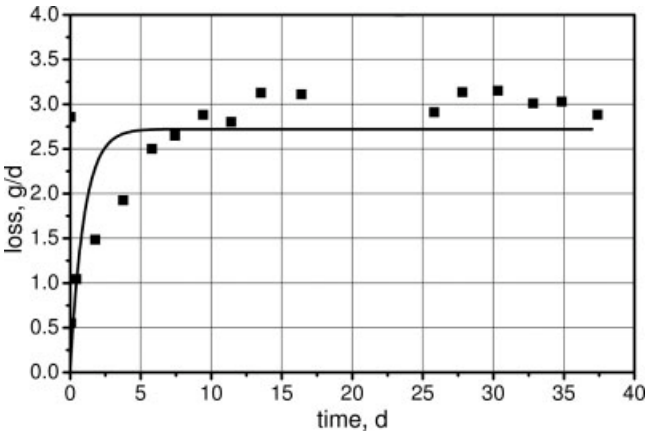

Figure 11. Development of the loss flux from the cyclone with time for the spent catalyst FCC-A, comparison of the measurements with the simulation.

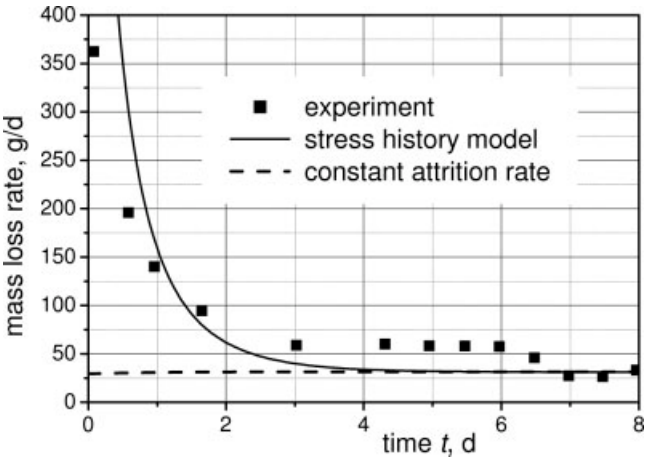

Figure 13. Development of mass loss with time for the fresh catalyst FCC-B at u = 0.45 m/s.

not clear, therefore, whether the first data point indicates a startup effect or simply is a measurement error.

Figure 12 presents the measured and calculated PSDs of the bed material and of the solids stream at the cyclone entrance. The samples for the PSD of the bed were withdrawn directly through the sample port of the bed, and the samples for determining the PSD of the solids entering the cyclone were collected via the suction probe located in the inlet duct to the cyclone. The PSD at the cyclone inlet was obtained by averaging four different samples taken at four different heights in the inlet duct to avoid measurement errors by particle segregation in the inlet flow. the samples were analyzed by laser diffraction (Beckmann Coulter LS 13320). The comparison between the measured and the calculated data shows a fairly good agreement and confirms that the model predicts the tendencies correctly. To get the best description of the experimental data the calculations could have been adapted to the experiments by fitting the model parameters. However, this has not been done here. The calculations are only based on parameters, which were obtained independently in the attrition tests or which like the entrainment parameters are given in the literature, respectively.

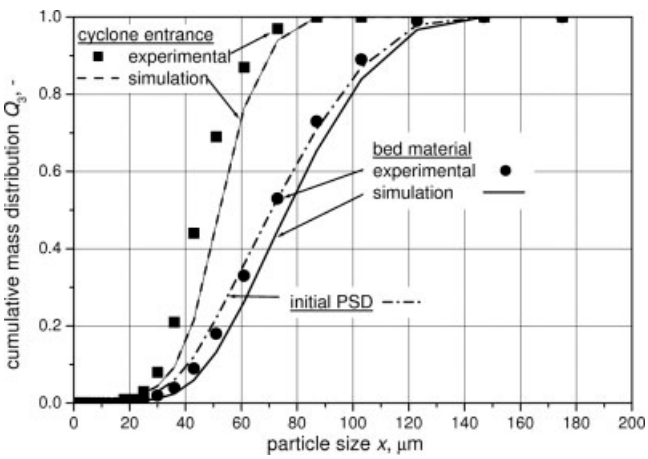

Figure 12. Particle-size distributions calculated for attrition of the spent catalyst FCC-A, and compared with PSDs of samples taken after 15 days from start.

For the second scenario the system was filled with fresh particles (FCC-B). Here the attrition behavior of the particles is changing with time as the particles have not undergone fluidizing conditions before. The particles were fluidized at a superficial velocity of 0.45 m/s with a cyclone inlet velocity of 13.4 m/s. The same sampling methods were applied as for the test with the spent particles FCC-A.

Figure 13 shows the development of the mass loss flux, which is observed in the overflow of the cyclone with time. The experimental data show a high-mass loss at the beginning, which is decreasing slowly over a period of eight days to reach a nearly constant rate. A first process simulation was carried out which neglected the increased attrition rate of fresh particles. The results, plotted as the dashed line, show that the loss mass flux is practically constant. With consideration of the increased attrition of fresh particles, the simulation with the full model describes the measured system behavior quite well. During the first days of operation the simulation predicts a higher mass loss flux than the actual measurements. Possible reasons for this deviation are the same as in the previous test run, that is, accumulation of fines in the bed and adhesion of fines to previously cleaned metal surfaces.

Conclusions

In this work an approach has been developed to predict the time-dependent changes of particle-size distributions in fluidized-bed systems with recirculation of solids. Several effects in fluidized bed systems are influencing the local PSD, and have been identified. They are grouped in separation and classification effects, transport effects and degradation effects of the individual particles. For separation and classification in the cyclone the Muschelknautz model[20] was used in this work.

While the separation effects depend on the momentary conditions only and not on the history of the particles, this is

not true for the attrition. Attrition has a strong effect on the particles, especially when fresh particles are applied, which have not undergone mechanical stress before. It has often been reported in the literature that fresh particles have a much higher-production rate of fines than particles, which have already been exposed to attrition stress for a long time. The attrition rate of fresh particles can be two to three-orders of magnitude higher than the attrition rate measured after a long time of exposure. This effect is referred to the condition of the particles surface. Fresh particles have a very rough surface with a lot of edges and small cracks. After a certain period of time exposed to abrasion these edges are rubbed off, and the particle surface gets smoothened. Then the attrition rate is governed by a natural roughness of the particles, which is depending on the inner structure of the individual particle.

From this finding it is concluded, that the stress experienced by the particles has to be monitored and taken into account in the modeling. The experienced stress is called here the "stress history" of the particles. In fluidized-bed systems with recirculation of solids the stress history is affected by attrition. Whenever a particle is exposed to one of the sources of attrition its stress history is changed, and this will influence the attrition behavior when it is, subsequently, subjected to another attrition mechanism. This illustrates a strong coupling of these sources. Even when two particles have been for the same time in the system they may have undergone different stress histories. For example, smaller particles will have been entrained and stressed in the cyclone more often than coarser ones.

In the approach chosen in this work a dimensionless stress history parameter ϑ is introduced, which defines the status of a particle at a certain moment. A stress history parameter ϑ below a certain limit means that a particle is not yet in a steady-state condition with respect to the attrition. For ϑ exceeding this limit the particle is in a state, where it will have the attrition behavior of a particle with of a fully smoothed surface. For the description of the attrition induced by one source, a set of two coefficients is needed, namely, the attrition coefficient and a reference for defining the stress history. For the unification of the description for all sources one parameter is needed to describe the shape of the stress history function $f(\vartheta)$. This parameter can be derived from experiments with isolated sources of attrition.

In order to describe a combination of fluidized beds and cyclones the model system is divided into modules, that is, one module for each apparatus in the system. In each module the changes in PSD, stress history, and the mass fluxes and PSD at the outlets are calculated, based on the previously mentioned models. The conditions at one module's outlet are used as the input to the subsequent module.

Two sets of experiments were carried out to examine the practical applicability of the simulation suggested here. In the first test case a spent FCC was fluidized in a bed/cyclone recirculation system, and the time-dependence of the solids flux lost through the cyclone overflow was monitored over a time span of 37 days. In a second run a fresh FCC was fluidized in the same plant for eight days days. In both cases the simulation is predicting the levels of attrition and the time histories of the loss flux, and of the PSD's in the system in good agreement with the measurements.

Acknowledgment

The authors would like to thank Jessica Schreiber who performed most of the measurements as part of her diploma thesis.

Notation

A_t = cross-sectional area of fluidized bed, m^2
b^* = exponent defined in Eq. 1
b = exponent defined in Eq. 26
C_b = particle-size independent rate constant of bubble-induced attrition, s^2/m^4
C_c = particle-size independent rate constant of cyclone attrition, s^2/m^3
C_j = particle-size independent rate constant of jet-induced attrition, s^2/m^3
d_{or} = diameter of an orifice in a multihole gas distributor, m
d_p = surface-mean diameter, m
D_t = diameter of fluidized bed, m
K_a = attrition coefficient in Eq.1
$k_{\infty,i}$ = mass fraction related entrainment flux of particles in size class i per unit bed area, $kg/m^2/s$
m_{att} = mass of abrasion-produced fines per one time step, kg
$\dot{m}_{att}$ = mass of abrasion-produced fines per unit time, kg/s
m_b = bed mass, kg
$m_{c,in}$ = mass entering the cyclone within one time step, kg
$\dot{m}_{c,in}$ = solids mass flux into the cyclone, kg/s
m_e = mass elutriated from a fluidized bed with the gas within one time step, kg
m_i = material mass in the size interval i, kg
$\dot{m}_{i,i-1}$ = mass-transfer flux due to particle shrinking from the size interval i to $(i-1)$, kg/s
m_j = mass of particles in stress-history class j, kg
$m_{j,j+1}$ = mass of particles traveling from stress-history class j to class j+1, kg
m_{loss} = mass lost from a given system through the cyclone overflow, kg
m_p = mass of a single particle, kg
m_p^* = mass of a single particle prior to attrition, kg
m_{tot} = total mass of all classes, kg
n_c^* = number of passes through cyclone, where $r_c = 1.1 \cdot r_{c,\infty}$, -
n_{or} = number of orifices in a multihole gas distributor
$Q_3(x)$ = cumulative particle size distribution in mass
$\Delta Q_{2,i}$ = fraction of the size interval i on the entire particle surface
$\Delta Q_{3,i}$ = fraction of the size interval i on the entire material mass
r = attrition rate, kg/kg/s
r^* = attrition rate of particles at t^* or n_c^*, kg/kg/s
Re = Reynolds number
t = time, s
t^* = time, where, $\dot{m}_{att} = 1.1 \cdot \dot{m}_{att}$, ∞, s
Δt = time interval, s
u = superficial-gas velocity, m/s
$u_{c,in}$ = gas velocity at the cyclone inlet, m/s
u_{mf} = minimum fluidization velocity, m/s
u_{or} = gas velocity in the orifice of a multihole gas distributor, m/s
w_s = terminal velocity of single particle, m/s
x = particle size, m
x_i^* = particle size which will travel from one size class i to the next size class $i-1$ by shrinkage, m
$\bar{x}_i$ = geometric mean-particle size of the size interval i, m

Greek letters

ϑ = stress history variable
$\Delta\vartheta$ = change of stress history variable within one time step or pass through a cyclone
ρ_f = density of gas, kg/m^3
ρ_s = density of particles, kg/m^3
$\mu_{c,in}$ = solids loading at the cyclone inlet
μ_{cr} = critical solids loading according to the critical load hypothesis for the Muschelknautz cyclone model
η_f = dynamic viscosity of gas, Pa s

Indices

i	=	particle size class
j	=	stress-history class or relating to jets
p	=	single particle
c	=	cyclone
b	=	bed or relating to bubbles
exp	=	under experimental conditions
tot	=	total of stress-history or total of all particles
∞	=	under steady-state conditions

Literature Cited

1. De Vries RJ, van Swaaij WPM, Mantovani C, Heijkoop A. Design criteria and performance of the commercial reactor for the shell chorine process. *Proc of the 5th Europ Symp on Chem React Eng*. Amsterdam: Elsevier; 1972:39–59.
2. Pell M, Jordan SP. Effects of fines and velocity on fluidized bed reactor performance. *AIChE Symp Ser*. 1988;84(262):68–73.
3. Cheng L, Chen B, Liu N, Luo Z, Cen K. Effect of characteristic of sorbents on their sulfur capture capability at a fluidized bed condition. *Fuel*. 2004;83:925–932.
4. Hilligardt K, Werther J. Influence of temperature and properties of solids on the size and growth of bubbles in gas fluidized beds. *Chem Eng Technol*. 1987;10:272–280.
5. Sit SP, Grace JR. Effect of bubble interaction an interphase mass transfer in fluidized beds. *Chem Eng Sci*. 1981;36:327–335.
6. Werther J, Hartge E-U. Modeling of industrial fluidized-bed reactors. *Ind Eng Chem Res*. 2004;43:5593–5604.
7. Forsythe WL, Hertwig WR. Attrition characteristics of fluid cracking catalysts. *Ind Eng Chem*. 1949;41:1200–1206.
8. Xi W. *Katalysatorabrieb in Wirbelschichtreaktoren*. Hamburg, Technical University Hamburg-Harburg; 1993. PhD thesis.
9. Reppenhagen J. *Catalyst attrition in fluidized bed systems*. Aachen: Shaker Verlag; 1999.
10. Werther J, Reppenhagen J. Attrition. In: Yang W-C, ed. Fluid-Particle Systems. New York: Marcel Dekker; 2003:201–237.
11. Gwyn JE. On the particle size distribution function and the attrition of cracking catalysts. *AIChE J*. 1969;15:35–38.
12. Pis JJ, Fuertes AB, Artos V, Suarez A, Rubiera F. Attrition of coal and ash particles in a fluidized bed. *Powder Technol*. 1991; 66:41.
13. Dessalces G, Kolenda F, Reymond JP. Attrition evaluation for catalysts used in fluidized or circulating fluidized bed reactors. AIChE: *Preprints of the First International Particle Technology Forum, Part II*. Denver, Colorado; 1994:190.
14. Werther J, Xi W. Jet attrition of catalyst particles in gas fluidized beds. *Powder Tech*. 1993;70:39.
15. Werther J, Reppenhagen J. Catalyst attrition in fluidized-bed systems. *AIChE J*. 1999;45(9):2001.
16. Reppenhagen J, Werther J. The role of catalyst attrition in the adjustment of the steady-state particle size distribution in fluidized bed systems. In: Kwauk M, Li J, Yang WC, eds. *Fluidization X*. New York: Engineering Foundation; 2001:69.
17. Werther J, Wein J. Expansion Behavior of Gas Fluidized Beds in the Turbulent Regime. *AIChE Symp. Ser. 90*. 1994;301:31–44.
18. Tasirin SM, Geldart D. Entrainment of FCC from fluidized beds – a new correlation for the elutriation rate constants. *Powder Technol*. 1998;95:240–247.
19. Trefz M, Muschelknautz E. Extended cyclone theory for gas flows with high solids concentration. *Chem Eng Technol*. 1993;16:153–160.
20. Muschelknautz E, Greif V, Trefz M. Zyklone zur Abscheidung von Feststoffen aus Gasen. VDI-Wärmeatlas. Duesseldorf: VDI Verlag; 1997:Lja 1–11.
21. Reppenhagen J, Werther J. Catalyst attrition in cyclones. *Powder Tech*. 2000;113:55.
22. Hartge E-U, Klett C, Werther J. Dynamic simulation of the particle size distribution in a circulating fluidized bed combustor. *Chem Eng Sci*. 2007;63:281–298.

Manuscript received July 14, 2006, and revision received Dec. 6, 2006.